

Molecular dynamics simulation of polymer nanoparticle collisions: orbital angular momentum effects

B.C. Hathorn^{a,*}, B.G. Sumpter^a, M.D. Barnes^b, D.W. Noid^a

^aOak Ridge National Laboratory, Division of Computer Science and Mathematics, Oak Ridge, TN 37831, USA

^bOak Ridge National Laboratory, Division of Chemical and Analytical Sciences, Oak Ridge, TN 37831, USA

Received 9 September 2001; received in revised form 10 December 2001; accepted 12 December 2001

Abstract

The collisional dynamics of polymer nanoparticles is investigated using molecular dynamics, with a particular focus on angular momentum effects. Unlike zero impact parameter collisions discussed elsewhere, which are greatly weighted toward sticking collisions, the outcome of collisions with non-zero angular momentum show much greater variability, showing both reactive (where polymer chains are exchanged between particles) and purely scattering trajectories. In the case of inelastic scattering trajectories, the profile for translation to vibration energy transfer is calculated. © 2002 Elsevier Science Ltd. All rights reserved.

Keywords: Angular momentum; Scattering trajectories; Collisional dynamics

1. Introduction

In recent years considerable effort has been underway in investigation of experimental and theoretical properties of polymer nanoparticles [1–24]. Since the development of techniques which allow precise manufacture of individual particles, the development of theoretical models which treat specific properties of individual particles, as opposed to treatments which examine average properties in the bulk, is becoming more important. Molecular dynamics provides a direct avenue to the investigations of these small systems.

Recently, experimental investigations of polymer micro- and nanoparticles have demonstrated formation of deterministic three-dimensional (3D) structures, including branched or linear chains of polymer particles, as well as closed rings [22]. These structures are highly stable and are being investigated for possible microphotronics and sensor applications. In the present work, we seek to investigate the interaction between polymer particles by modeling the collisional dynamics of the particles, which result in the superparticle structures.

Collisions between molecules are an inherently important phenomenon in chemistry. Ultimately, collisions control chemical kinetics and dynamics observed in molecular interactions. Much of the focus in the past has been in the

close interactions between small molecules, and a large amount of information has been obtained, including such information as the translation to vibration energy transfer, and the lifetimes of collision complexes formed [25,26]. Molecular dynamics simulations have been employed to study atomistic nanoparticles [27–32], however these particles consisted of clusters of small atoms which would have relatively free migration within the final composite structure, and allow for (relatively) rapid coalescence which minimizes the surface energy with respect to the volume. It is clear that in the present case, where the polymer nanoparticles retain much of their initial structure [22], the transport of individual units within the cluster must be limited by the presence of chain structure within the particles.

In an inelastic close encounter of two molecular species there are ultimately three possible outcomes: the molecules can ‘stick’ and remain tightly bound after the collision if enough of the energy is removed from the translational coordinate so that it has insufficient energy to redissociate; the molecules can scatter, when the amount of energy transferred from the relative translational coordinate to the internal coordinates leaves enough energy in the relative translational coordinate for the molecule to redissociate; and the molecules can react or undergo a fundamental change in structure prompted by the near interaction and the surplus of energy obtained from the relative translational coordinate.

* Corresponding author.

E-mail address: bryan@kennel.caltech.edu (B.C. Hathorn).

In previous work, we have elucidated these regimes in the case of collinear collisions of polymer particles [23]. In that work, we found that at low velocities the particles would stick, and at high relative velocities the particles would indeed react, but that the nature of the reaction was to alter the structure of the incident particles, either by exchanging polymer chains between the particles, or by splitting off particle fragments.

In the current paper, we extend the treatment to collisions of polymer particles where there is a component of orbital angular momentum. In the present case, the role of angular momentum is clear, as one expects that in large impact parameter (high angular momentum) collisions, the collisions will only be glancing ones, and so the probability of scattering trajectories where there is translational to vibrational energy transfer but particles retain their initial composition, is enhanced.

Typically, for collisions of small molecules, the usual approach is to assume that the potential between the interacting molecules can be considered as roughly spherically symmetric and is only dependent on the relative separation of the two species [25,26]. In this two body central force approximation, the classical dynamics of the trajectories can be solved exactly.¹ Essentially, the problem of incorporating angular momentum is accounted for by replacing the two-body potential $V(r)$, with a fictitious effective potential, $V'(r)$:

$$V'(r) = V(r) + \frac{l^2}{2\mu r^2}. \quad (1)$$

Here, $l = \mu v b$ is the angular momentum, with μ the two-body reduced mass, v the initial velocity, b is the impact parameter, and r is the relative separation between the two masses. Essentially, the entire motion is now represented as a 1D problem, which involves only the separation between two structureless particles. We note that such an approximate treatment has been demonstrated to be effective over a wide range of systems, from planetary motion in celestial mechanics, to scattering of alpha particles in the classic Rutherford scattering experiment [33].

In the present case, however, a complication arises which prevents the application of the simple 1D analysis. Unlike the case of planetary bodies in celestial mechanics or the attraction between small particles or molecules, in the present case the two-body potential can have significant changes due to the internal reorganization of the polymer particles over the timescale of the collision, due to the molecular dynamics of the bodies [23]. In the former case, the effective potential is solely a function of the fixed central

¹ It is noteworthy to remark here that classical trajectories are deterministic in nature, and thus conflict with the quantum mechanical picture, where the uncertainty relation of Heisenberg must remain in force. Nonetheless, since the particles in the present calculation are massive in comparison with the usual quantum scale, we presuppose that a classical mechanics picture is valid.

force potential and the angular momentum. In the present case, the central force potential is no longer fixed (and may, in fact, show some variability with angular variation, since the polymer particles are not perfect spheres), there may be significant conversion of translational to vibrational energy, or even reactions, which change the nature of the particles in question. Nonetheless, the interpretation of collisions of nanoparticles in the context of the well-established central force formalism is worthwhile.

In Section 2, we review the basic principles and methods utilized in the molecular dynamics simulation of particle collisions. In Section 3, we describe the results of the simulations performed, and in Section 4 we discuss the results.

2. Simulation methodology

For the purposes of the present study, we have examined motions and interaction forces between individual polymer particles both before and after interactions take place. The method of the calculations corresponds to a classical mechanical simulation. The details of the computations involving the geometric statement function approach are described more fully elsewhere [34] and are presented concisely here.

In previous efforts from our group (see for example, Refs. [1–23]) polymer chains confined to small ($d \approx l$ where d is the particle diameter and l is the chain length) 3D geometries have been studied experimentally and treated with a molecular dynamics approach [35,36], integrating Hamilton's equations of motion in time,

$$q_i = \frac{\partial H}{\partial p_i}, \quad (2)$$

$$-p_i = \frac{\partial H}{\partial q_i}, \quad (3)$$

where H is the Hamiltonian of the system and the q_i and p_i represent the coordinates and their conjugate momenta. In the present case, we have treated coordinates and momenta in the Cartesian frame, where the total kinetic energy is diagonal.

For simplicity of the polyethylene model, we have collapsed the CH₂ and CH₃ units into a single monomer of mass 14.5 amu. By neglecting the internal structure of these groups, the number of coordinates and thus the number of equation of motion for the system are reduced. The model has been shown to be useful to study the low temperature behavior of the system where the effects of the hydrogens have little effect on the heat capacity and entropy of the system [38].

The Hamiltonian for the system is specified as:

$$H = T + \sum V_{2b} + \sum V_{3b} + \sum V_{4b} + \sum V_{nb}, \quad (4)$$

where T is the kinetic energy component, expressed in terms of Cartesian coordinates, and the terms V_{2b} , V_{3b} and V_{4b} represent the two-, three-, and four-body terms for monomer units in an individual polymer strand, and V_{nb} is the non-bonded interaction between individual monomer units separated by four or more monomer units along the chain (flexibility in the chains allows for the chains to bend back to have close contact) or between monomer units in different chains, within a spherical cutoff of 10 Å. The functional forms of the potentials are given by [38–42]:

$$V_{2b} = D\{1 - \exp[-\alpha(r_{ij} - r_e)]\}, \quad (5)$$

$$V_{3b} = \frac{1}{2} \gamma (\cos \theta - \cos \theta_e)^2, \quad (6)$$

$$V_{4b} = 8.77 + a \cos \tau + b \cos^3 \tau, \quad (7)$$

$$V_{nb} = 4\epsilon \left[\left(\frac{\sigma}{r_{ij}} \right)^{12} - \left(\frac{\sigma}{r_{ij}} \right)^6 \right], \quad (8)$$

with the values of the constant terms given in Table 1. The distances between the various monomer units, r_{ij} are given by the standard Cartesian relation,

$$r_{ij} = \sqrt{(x_i - x_j)^2 + (y_i - y_j)^2 + (z_i - z_j)^2}. \quad (9)$$

In the present case, initial conditions for the trajectories comprised the coordinates of individual polymer particles, which had previously been obtained by an annealing [14], with momenta chosen randomly in the radial coordinate so as not to excite any internal angular momentum. The randomly chosen momenta were rescaled so as to produce

the appropriate temperature for the simulation,

$$\sum_i \frac{1}{2m_i} p_i^2 = \frac{3}{2} k_B T, \quad (10)$$

where T is the absolute temperature and k_B is Boltzmann's constant.

The thermalized particles were offset in the z -coordinate, and given an initial relative velocity in the z -coordinate so as to produce a collision. Orbital angular momentum was introduced by the use of a variable impact parameter, b , chosen as a displacement in the x direction. The angular momentum is then given by $L = \mu v b$ where μ represents the reduced mass of the particle pair, v is the velocity in the z direction, and b is the x coordinate offset. The initial z offset was chosen so as to give at least 1 ps of time for the particles thermally equilibrate before coming within the maximum range of forces with the other particle (in the present case, 10 Å). Integration of the equations of motion was accomplished by use of novel symplectic integrators developed in our laboratory [37].

A number of properties were tracked during the course of the simulation. Principal among them were the positions and velocities of the centers of mass of the particles, the center of mass separation of the two particles, and the moments of radial distribution of the particles. The first two give the time development of the positions and distances of the particles, the last gives a measure of the particle integrity (when polymer chains are exchanged between the particles or become detached from the parent particle, the average distance of the monomer units from the center of mass becomes large). We note that in the following discussions, the relative velocity is the velocity between the two particle centers of mass.

3. Results

A number of trajectories were run for collisions of particles with of 30 chains composed of 100 monomer units. Various initial conditions for the impact parameter and relative velocities of the particles were assumed, with internal temperatures being chosen to be near absolute zero. The classification scheme for the results of the trajectories is outlined below. A summary of the trajectory outcomes is represented in Fig. 1.

3.1. Sticking trajectories

During the course of the simulation, trajectories were deemed to result in particle sticking if the resultant separation in the center of mass of the two initial particles became bounded and remained so for the whole of the simulation timescale. At the same time, the particles maintained their integrity, with no parts of the particles becoming dissociated from the parent, as

Table 1
Potential parameters for polyethylene particle systems

Two-body bonded constants^a

$D = 334.72$ kJ/mol

$r_e = 1.53$ Å

$\alpha = 199$ Å⁻¹

Three-body bonded constants^b

$\gamma = 130.122$ kJ/mol

$\theta_e = 113^\circ$

Four-body bonded constants^a

$a = -18.4096$ kJ/mol

$b = 26.78$ kJ/mol

Two-body non-bonded constants^a

$\epsilon = 0.4937$ kJ/mol

$\sigma = 4.335$ Å

^a Refs. [41,42].

^b Refs. [39,40].

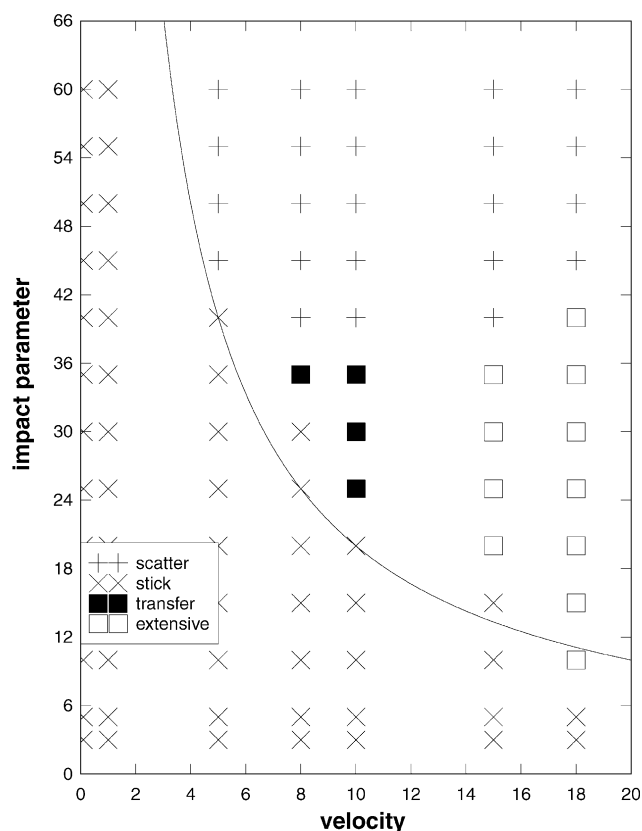


Fig. 1. Classification of sticking and reactive trajectories as a function of relative velocity (Å/ps) and impact parameter (Å).

would characterize a ‘reactive trajectory’, described in Section 3.2. The time dependence of the center of mass separation of a typical sticking trajectory is represented in Fig. 2.

3.2. Reactive trajectories

A large number of trajectories were observed to be ‘reactive’ in that one or both of the particles lost its structure, and fragments of the particle became dissociated from the parent during the course of the trajectory. A straightforward measure of the reaction of the particles is evidenced by the average value of the square of the radial distribution,

$$\langle r^2 \rangle = \frac{1}{N} \sum_{i=1}^N (x_i - x_{CM})^2 + (y_i - y_{CM})^2 + (z_i - z_{CM})^2, \quad (11)$$

where (x_i, y_i, z_i) are the positions of the monomer units making up the particle, and (x_{CM}, y_{CM}, z_{CM}) is the position of the center of mass. Reaction of a particle leads to a value of $\langle r^2 \rangle$ which is unbounded as time progresses. A comparison of the time dependence of the $\langle r^2 \rangle$ is shown in Fig. 3 for typical reactive and unreactive trajectories.

The nature of the reaction is determined by an analysis of

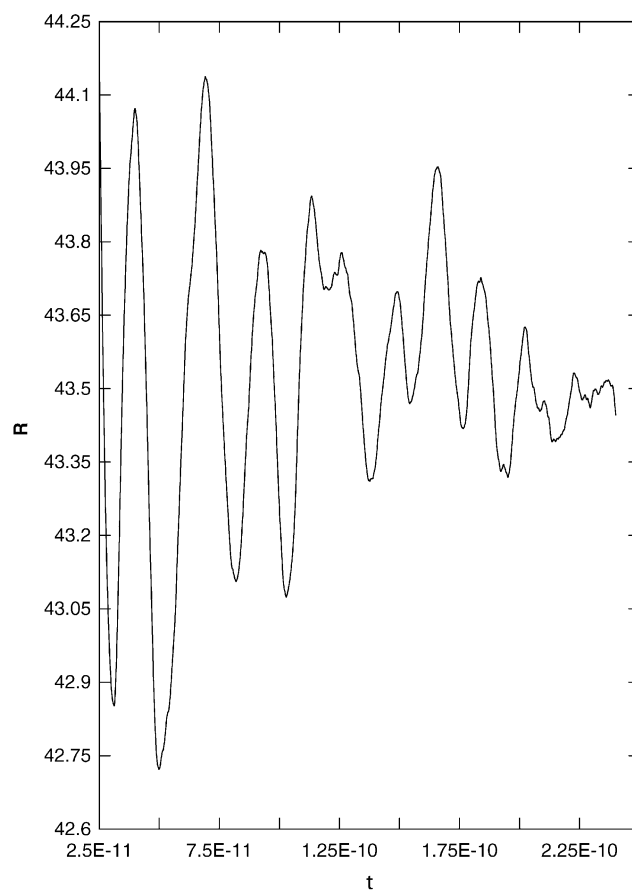


Fig. 2. Time dependence (s) of the center of mass separation, R (Å) in a typical ‘sticking’ trajectory. In this case, the particles were composed of 30 chains (100 monomers each), with internal temperature of 5 K, zero impact parameter, and an initial relative velocity of 1 Å/ps.

positions of the monomer units. In general, two types of reactions can occur, reactions where a particle is shattered and pieces break off, and trajectories where the reaction consists of an exchange of matter between two colliding particles. There is a certain amount of subjectivity in the classifications, for the purposes of this study we have classified trajectories where at most a single chain is transferred from one particle to another as ‘transfers’ and trajectories where more than a single chain is transferred, or the particle is broken into smaller pieces as ‘extensive’. Examples of the two kinds of reactive trajectories are shown in Figs. 4 and 5.

3.3. Scattering trajectories

A determination was made that a trajectory could be characterized as a scattering trajectory if at the conclusion of the 100 ps simulation, center of mass separation of the particles was increasing, and the distance of separation of the nearest monomer units in the two particles was more than 10 Å (the cutoff of the Lennard Jones non-bonded interactions), leading to no possibility of return. At the

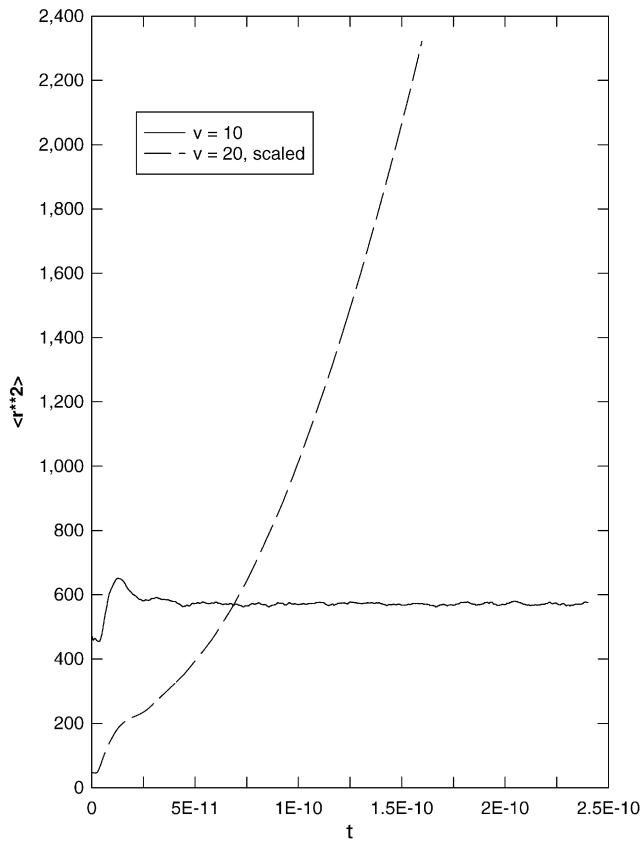


Fig. 3. Time dependence of $\langle r^2 \rangle$ for typical reactive and unreactive trajectories. Initial relative collision velocities are 10 and 20 Å/ps, respectively, with zero impact parameter. The curve for the 20 Å/ps collision has been scaled by a factor of 0.1 so as to fit on the same axes. Only one particle is shown for each collision.

same time, however, the particles must maintain their integrity, so $\langle r^2 \rangle$ must remain bounded for both particles. For scattering trajectories, the conversion of relative translational energy to internal vibrational energy was calculated, and is represented in Fig. 6.

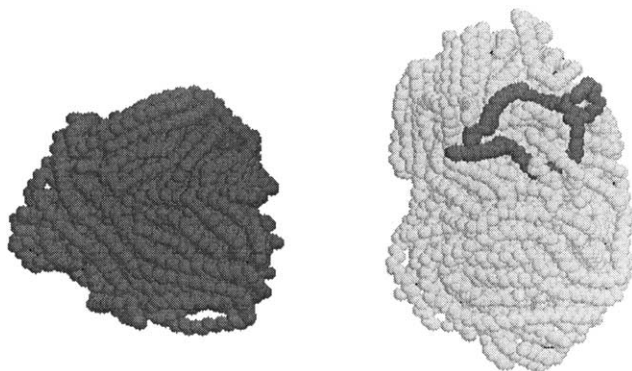


Fig. 4. Final configuration for a transfer type reactive scattering collision. The initial conditions for the trajectory had a relative velocity of 10 Å/ps, with an impact parameter of 30 Å, and an internal temperature of 5 K. Coordinate axes have been rotated to best present the transferred chain.

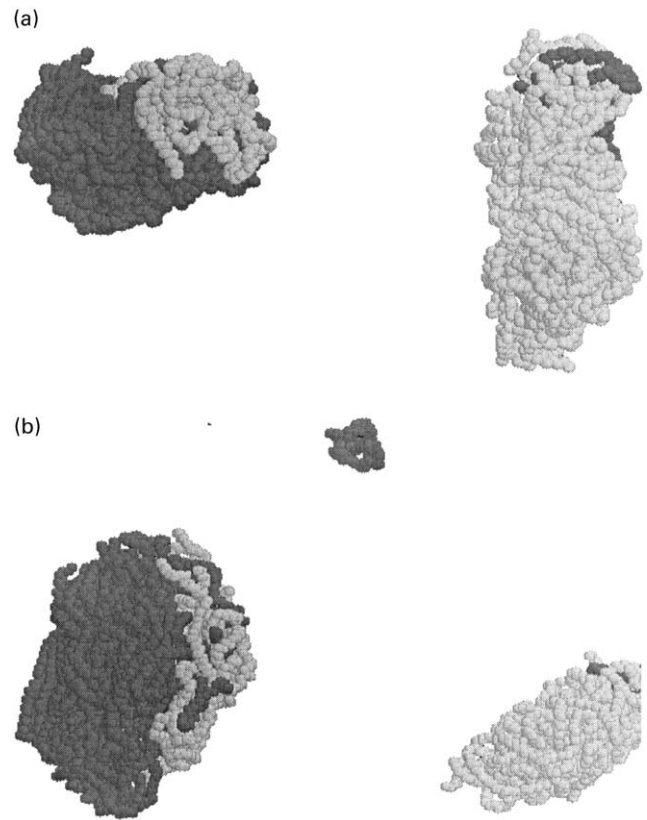


Fig. 5. Final configurations for two ‘extensive’ reactive collisions: (a) Exchange of a substantial number of chains between particles, and (b) loss of particle integrity. Coordinate axes have been rotated to best present the reacted particles.

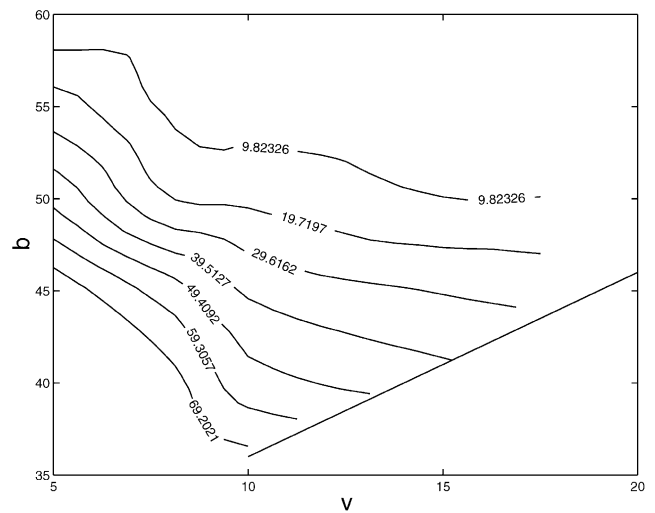


Fig. 6. Conversion of relative translational energy to internal vibrational energy as a function of initial velocity, v (Å/ps) and impact parameter, b (Å). Contours are percent of relative translational energy converted, and are obtained by a cubic interpolation to the scattering data in Fig. 1. The solid line making up the right hand border is the approximate boundary between reactive and scattering collisions.

4. Discussion

Examination of the velocity-impact parameter distribution for the polymer particle collisions demonstrates that even though the interparticle potential is not independent of the time, and varies with the relaxation of the particles, it is possible to consider the dynamics by considering the usual central force picture, with some modifications to account for the fact that the particles cannot be treated as point particles, and exhibit manifestations of internal structural change during the collision process.

It is apparent from the outcome of the collisions that angular momenta less than approximately $4.35 \times 10^6 \text{ \AA}^2 \text{ amu/ps}$ (represented by the solid line in Fig. 1) lead to irreversible sticking of the particles. In a schematic representation of the effective potential for the central force problem, this outcome likely derives from penetration to the inner core, beyond the effective barrier maximum. The translation to vibration energy exchange is quite efficient, due to the high number of vibrational normal modes, effectively causing relaxation and stabilization of the collision pair into a dimerized particle.

At angular momenta larger than this value, however, the particles are repelled from the outer barrier. Such a collision transfers the translational energy into internal energy, but if sufficient energy is available from the translational coordinate, it may surmount the barrier necessary for a reactive event, initiating a transfer of matter from one particle to another, or in the event that a large amount of energy is available, a particle may be fragmented.

The availability of relative translational energy for reactive processes is illustrated by the transfer of translational energy into vibrational (internal) energy in the course of a collision. For collisions which represent true scattering collisions, i.e. those which do not react or stick, the final translational energy can be determined from relative velocities of the centers of mass of the two particles. The fraction of the relative translational energy which has been converted to internal energy is represented in Fig. 6. It is immediately apparent that there is no quantized energy transfer, as one might expect in small molecules, nor should we expect there to be any, as the present simulation only accounts for the evolution of the classical mechanical equations of motion. Nonetheless, we expect that the description of the energy transfer should closely mimic that of the actual system, as the particles have a very large density of states, and there is a near continuum of states available for energy transfer.

At the same time, however, we expect that during the course of the simulation the energy may become concentrated in the low frequency modes, resulting in 'too much classical chaos', as has been observed in a number of other computational experiments [43]. Essentially, this effect arises from the failure of the system to properly treat the zero-point energy. The accessibility of the zero-point energy in classical mechanical simulations has been

shown elsewhere to contribute to enhancement of the rate constants and other non-physical effects [44]. Such rapid relaxation of the zero-point energy may indeed contribute to the great propensity of the particles to deform, despite the relatively low initial temperatures in the present study.

In conclusion, we present here the first study of orbital angular momentum effects in polymer nanoparticles. In contrast to collinear collisions [23], collisions with a non-zero impact parameter show a wide variety of possible outcomes, ranging from sticking collisions, to reactive and scattering collisions. It is demonstrated that in the classical mechanical simulations, the conversion of relative translational energy to internal vibrational energy is very efficient, owing in part to the inaccuracy of molecular dynamics simulations to properly treat the zero-point energy, but also to the very large and essentially continuous density of states. As was observed elsewhere [23] it is the very rapid conversion of translational to vibrational energy which facilitates sticking collisions except at very large relative translational energies.

Acknowledgements

This work was sponsored by the Division of Computer Science and Mathematics and the Division of Materials Sciences, Office of Basic Energy Sciences, US Department of Energy under Contract DE-AC05-00OR22725 with UT-Battelle at Oak Ridge National Laboratory (ORNL), using resources of the Center for Computational Sciences at Oak Ridge National Laboratory. One of us (BCH) has been supported by the Postdoctoral Research Associates Program administered jointly by ORNL and the Oak Ridge Institute for Science and Education.

References

- [1] Kung C-Y, Barnes M, Sumpter BG, Noid DW, Otaigbe J. Polym Preprint 1998;39:610.
- [2] Barnes MD, Kung C-Y, Sumpter BG, Noid DW, Otaigbe J. Optics Letts 1999;24:121.
- [3] Barnes MD, Ng KC, Fukui K, Sumpter BG, Noid DW. Mater Today 1999;2:25.
- [4] Barnes MD, Ng KC, Fukui K, Sumpter BG, Noid DW. Macromolecules 1999;32:7183.
- [5] Ford JV, Sumpter BG, Noid DW, Barnes MD. Chem Phys Lett 2000;316:181.
- [6] Ford JV, Sumpter BG, Noid DW, Barnes MD. J Phys Chem B 2000;104:495.
- [7] Ford JV, Sumpter BG, Noid DW, Barnes MD. Polymer 2000;41:8075.
- [8] Ford JV, Sumpter BG, Noid DW, Barnes MD, Otaigbe JU. Appl Phys Lett 2000;77:2515.
- [9] Otaigbe J, Barnes M, Fukui K, Sumpter BG, Noid DW. Adv Polym Sci 2001;154:1.
- [10] Fukui K, Sumpter BG, Barnes M, Noid DW, Otaigbe J. Polym Preprint 1998;39:612.
- [11] Fukui K, Sumpter BG, Barnes MD, Noid DW, Otaigbe J. Macromol Theory Simulat 1999;8:38.

- [12] Fukui K, Sumpter BG, Runge K, Kung CY, Barnes M, Noid DW. *Chem Phys* 1999;244:339.
- [13] Fukui K, Sumpter BG, Barnes MD, Noid DW. *Comput Theoret Polym Sci* 1999;9:245.
- [14] Fukui K, Sumpter BG, Barnes MD, Noid DW. *Polym J* 1999;31:664.
- [15] Noid DW, Fukui K, Sumpter BG, Yang C, Tuzun R. *Chem Phys Lett* 2000;316:285.
- [16] Fukui K, Noid DW, Sumpter BG, Yang C, Tuzun R. *J Phys Chem B* 2000;104:526.
- [17] Sumpter BG, Barnes MD, Fukui K, Noid DW. *Mater Today* 2000;2:3.
- [18] Fukui K, Sumpter BG, Yang C, Noid DW, Tuzun RE. *J Polym Sci: Polym Phys* 2000;38:1812.
- [19] Fukui K, Sumpter BG, Barnes MD, Noid DW. *Macromolecules* 2000;33:5982.
- [20] Sumpter BG, Fukui K, Barnes MD, Noid DW. *Computational studies, nanotechnology, and solution thermodynamics of polymer systems*. Dordrecht/New York: Kluwer Academic Publishers/Plenum Press, 2001.
- [21] Fukui K, Sumpter BG, Yang C, Noid DW, Tuzun RE. *Comput Theoret Polym Sci* 2001;11:191.
- [22] Barnes MD, Mahurin S, Mehta A, Sumpter BG, Noid DW. Submitted for publication.
- [23] Hathorn BC, Sumpter BG, Barnes MD, Noid DW. Submitted for publication.
- [24] Vao-soongern V, Ozisik R, Mattice WL. *Macromol Theory Simulat* 2001;10:553.
- [25] Child MS. *Molecular collision theory*. Mineola, NY: Dover Publications, 1996 and references therein.
- [26] Levine RD, Bernstein RB. *Molecular reaction dynamics and chemical reactivity*. New York: Oxford University Press, 1987 and references therein.
- [27] Lehtinen KEJ, Zachariah MR. *Phys Rev B* 2001;63:205402.
- [28] Zachariah MR, Carrier MJ. *J Aerosol Sci* 1999;30:1139.
- [29] Zhu HL, Averback RS. *Mater Manufact Proc* 1996;11:905.
- [30] Zhu HL, Averback RS. *Philos Mag Lett* 1996;73:27.
- [31] Blasiten-Barojas E, Zachariah MR. *Phys Rev B* 1992;45:4403.
- [32] Gay JG, Berne BJ. *J Colloid Interf Sci* 1986;109:90.
- [33] Goldstein H. *Classical mechanics*. Reading, MA: Addison-Wesley, 1980 and references therein.
- [34] Noid DW, Sumpter BG, Wunderlich B, Pfeffer GA. *J Comput Chem* 1990;11:236.
- [35] Hoover WG. *Annu Rev Phys Chem* 1983;34:103.
- [36] Klein ML. *Annu Rev Phys Chem* 1985;36:525.
- [37] Gray SK, Noid DW, Sumpter BG. *J Chem Phys* 1994;101:4062.
- [38] Sumpter BG, Noid DW, Wunderlich B. *J Chem Phys* 1990;93:6875.
- [39] Weber TA. *J Chem Phys* 1978;69:2347.
- [40] Weber TA. *J Chem Phys* 1979;70:4277.
- [41] Sorensen RA, Liam WB, Boyd RH. *Macromolecules* 1988;21:194.
- [42] Boyd RH. *J Chem Phys* 1968;49:2574.
- [43] Tuzun RE, Sumpter BG, Noid DW. *Macromol Theory Simulat* 1998;7:203 and references therein.
- [44] Hathorn BC, Sumpter BG, Noid DW. *Polymer* 2002 in press.